Chemico-Biological Interactions 183 (2010) 133–141

Contents lists available at ScienceDirect

Chemico-Biological Interactions

journal homepage: www.elsevier.com/locate/chembioint

XJW20, a novel oxoindole derivative, induces G2/M arrest and apoptosis selectively in K562 leukemia cell line

Ziqi Ye[a,c], Zhe Chen[a], Wenteng Chen[b], Jinwen Xie[b], Hongyu Yang[a], Yijia Lou[a,*], Yongping Yu[b,**]

[a] Institute of Pharmacology, Toxicology and Biochemical Pharmaceutics, Zhejiang University, Hangzhou, 310058, China
[b] Institute of Materia Medica, Zhejiang University, Hangzhou, 310058, China
[c] Department of Pharmacy, The First Affiliated Hospital, College of Medicine, Zhejiang University, Hangzhou, 310003, China

ARTICLE INFO

Article history:
Received 15 September 2009
Received in revised form 20 October 2009
Accepted 20 October 2009
Available online 31 October 2009

Keywords:
Oxoindole derivate
Antitumor
K562 cell line
G2/M arrest
Apoptosis
Mitochondrial transmembrane potential

ABSTRACT

In comparison with four tumor cell lines and three non transformed cell types, chronic myeloid leukemia K562 cells were selectively sensitive to proliferation inhibition by the oxoindole derivative XJW20, as determined by the MTT assay. Further investigation revealed that XJW20 selectively induced G2/M arrest and apoptosis in K562 cells. At the molecular level, XJW20-induced G2/M arrest was accompanied by up-regulation of cyclin B1 and phospho (p)-Cdc25C (Ser216) and down-regulation of CDK1. There is no change in the expression of CDK2. The increased apoptotic activity by XJW20 was characterized by an increase in reactive oxygen species (ROS) generation, the mitochondrial transmembrane potential ($\Delta\Psi_m$) dissipation, cytochrome C releasing, apoptotic nuclei (AO/EB double staining) and nuclei condensation (DAPI-staining). The down-regulation of phosphorylated ERK was also found in XJW20-treated K562 cells. These molecular events induced by XJW20 may provide insight into the mechanism of action that led to growth arrest and apoptosis.

1. Introduction

Cyclin-dependent kinases (CDKs) are key elements of the cell-cycle progression. CDKs and their associated molecule elements have been considered as potential targets for anticancer drug discovery [1–3]. Compounds with an oxoindole parent structure (Fig. 1, Structure A) were expected to selectively regulate CDKs, and many potent CDK2 oxoindole inhibitors have been reported [4,5]. Therefore, we designed and synthesized a series of novel oxoindole derivates to identify compounds that may serve as an anticancer therapeutics. XJW20, 3-(3,4,5-trimethoxybenzylidene)-5-carboethoxy-indolin-2-one (Fig. 1, Structure B), was found to selectively inhibit the proliferation of K562 chronic myelogenous leukemia cell line among myeloid and somatic cell lines.

It has been demonstrated that inhibition of CDK4/6, CDK2, and CDK1 frequently results in arrest at the G1/S and G2/M boundaries. CDK1 inhibition may augment cell death after mitotic checkpoint activation by taxanes or kinesin spindle protein inhibitors [1]. In comparison, highly selective CDK2 inhibition does not have antiproliferative effects in many cancer cell types [1]. Studies have shown that initiation of G2 arrest in response to DNA damage through phosphorylation of Cdc25C on the serine-216 (Ser216) residue, a primary regulator is critical for G2 checkpoint regulation [6,7]. The activity of Cdc25C is well known to be negatively regulated by phosphorylation of Cdc25C on Ser216. It has been reported that compounds, such as protoapigenone, could induce G2/M arrest by modulating the levels of CDK2 and p-Cdc25C (Ser216) [8]. One of the network-complexes that regulate the G2 to M transition has now been revealed to be a Cdc25C-cyclin B1/Cdc2 controlled switch-like system. At the onset of mitosis, the complexes of cyclin B1/Cdc2 become active when the dual specificity phosphatase, Cdc25C, removes inhibitory phosphorylations on Cdc2 [9]. Moreover, the pathway to initiate the prolonged G2/M delay in HCT116 was different from the DNA damage checkpoint pathway, which is activated through the phosphorylation of Chk1/p-Cdc25C (Ser216) [9]. Present work, therefore, focused on both CDK1 and CDK2 expressions [10] or cyclin B1 and phospho (p)-Cdc25C expressions.

Moreover, we evaluated the underlying mechanisms involved in apoptosis of K562 cells treated with XJW20. Recent investigations have demonstrated that the mitochondrial dysfunction is involved in apoptosis [11]. An increase of reactive oxygen species (ROS) [12] and a consequent loss of mitochondrial membrane potential

* Corresponding author at: Institute of Pharmacology, Toxicology and Biochemical Pharmaceutics, College of Pharmaceutical Sciences, Zhejiang University, 388 Yuhangtang Road, Hangzhou, 310058, China. Tel.: +86 571 88208403; fax: +86 571 88208403.
** Corresponding author at: Institute of Materia Medica, College of Pharmaceutical Sciences, Zhejiang University, Hangzhou 310058, China. Tel.: +86 571 88208451.
E-mail addresses: yijialou@zju.edu.cn (Y. Lou), yyu@zju.edu.cn (Y. Yu).

0009-2797/$ – see front matter © 2009 Elsevier Ireland Ltd. All rights reserved.
doi:10.1016/j.cbi.2009.10.015

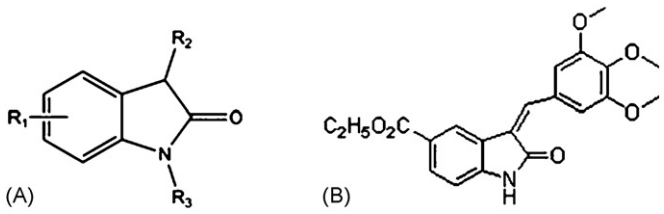

Fig. 1. Chemical structure of oxindole (A) and 3-(3,4,5-trimethoxybenzylidene)-5-carboethoxy-indolin-2-one (XJW20) (B). Structure (B) R_1, $-CO_2C_2H_5$; R_2, 3-(3,4,5-trimethoxybenzylidene).

($\Delta\Psi_m$) were reported as typical phenomena in the process of apoptosis related to mitochondria [13].

Molecular events, such as phosphorylation status of ERK, were also explored. Mitogen-activated protein kinases (MAPKs) are proline-directed Ser/Thr protein kinases and regulate many cellular processes including cell proliferation, migration, differentiation, and death. Three subfamilies of MAPKs, comprising c-Jun N-terminal protein kinase (JNK), extracellular signal regulating kinase (ERK) and p38 MAPK, have been identified and are activated by their upstream MAPK kinase (MKK). The MAPK pathway has been implicated in the response of tumor cells to chemotherapeutic drugs, such as taxol, etoposide and cisplatin, suggesting that the MAPK pathway may be a promising target for anticancer drugs. Additionally, the ERK MAP kinase is directly involved in activating Cdc25C during the G2/M transition [11].

In this study, we investigated the mechanisms of action of XJW20 by probing these molecular events that are involved in both cell-cycle progression and apoptosis.

2. Materials and methods

2.1. Cell lines and reagents

Neoplastic cell lines K562, PC-3, MCF-7, A549, and HO8910 were obtained from the Chinese Academy of Science (China). Endothelial cell line EA.hy926 was the kind gift of Professor Edgell at the University of North Carolina at Chapel Hill (NC, USA). Mouse embryonic fibroblasts (MEF) were prepared from fetus obtained from the mouse on d 13 of gestation [14]. The human purified leukocytes were freshly isolated from healthy volunteers as literature described [15] according to rules of the Ethics Committee at Zhejiang University. MCF-7 cell line and MEF cells were maintained in DMEM (Gibco, Grand Island, NY, USA). Other cell lines were cultured in RPMI 1640 medium (Gibco, Grand Island, NY, USA) with 10% heat-inactivated newborn calf serum (Hangzhou Sijiqing Biological Engineering Materials Co. China), 100 IU/mL penicillin, and 100 μg/mL streptomycin at 37 °C with 5% CO_2. XJW20 was synthesized by the Institute of Materia Medica at Zhejiang University.

DMSO and 3-(4,5-dimethylthiazol-2-yl)-2,5-diphenyltetrazolium bromide (MTT) were purchased from Sigma–Aldrich (St. Louis, MO, USA). The mitochondrial fluorescent probe 5,5′,6,6′-tetrachloro-1,1′,3,3′-tetra-ethylbenzimidazol-carbocyanine iodide (JC-1) and the 5-(and-6)-carboxy-2′-7′-dichlorofluorescin diacetate (carboxy-DCFDA) were purchased from Molecular Probes (Eugene, OR, USA). Fluorescent DNA-binding dyes acridine orange (AO)/ethidium bromide (EB) and propiaium iodide (PI) were obtained from Fluka (Switzerland). 4,6-Diamidino-2-phenylindole (DAPI) was obtained from Grand Island (NY, USA). Stock solutions of JC-1 (2 mg/mL), DAPI and carboxy-DCFDA (15.0 mmol/L) were dissolved in DMSO and stored at −20 °C. Primary antibodies against CDK1, CDK2, cyclin B1 were purchased from Boster Biological Technology Ltd. (Wuhan, China), p-cdc25C (Ser216) from Epitomics Biological Technology Co. Ltd. (China) and primary antibodies against ERK1/2, p-ERK1/2, cytochrome C (Cytosol), GAPDH, HRP-labeled secondary anti-mouse, anti-rabbit antibodies were purchased from Santa Cruz Biotechnology (CA, USA).

2.2. Cell viability assays

Viability assays were done using the MTT assay. Cell lines were plated at a density of 5×10^4 cells per well on 96-well plates in 100 μL of culture medium. XJW20 was added to a final concentration between 0.01–100 μmol/L for 72 h. Then MTT labeling mixture (50 μL, 5 mg/mL) was added to each well and incubated for an additional 4 h. The formazan precipitate was dissolved in 150 μL dimethyl sulfoxide and measured with a DTX-880 Multimode Detector (Beckman Coulter, USA) at 570 nm. Assays were performed in triplicate in three independent experiments. The concentration of compound needed to cause 50% growth inhibition (IC_{50}) was calculated against untreated cells using the dose–effect analysis software installed on the microcomputers.

2.3. Cytomorphological evaluation by phase contrast microscopy

The selectivity of cytotoxicity of XJW20 on K562 cell line was also evaluated. K562 cell line, EA.hy926, primary cultured human leukocytes and MEF were incubated with XJW20 (0.2–0.8 μmol/L) for 48 h as described above. Then the cells appearance were observed under an inverted phase-contrast microscope (Leica DMIL) and recorded using a Leica CCD camera (DC200) (Leica Microsystems Wetzlar, Germany).

2.4. Morphological evaluation by fluorescent microscopy

For mitochondrial membrane potential ($\Delta\Psi_m$) detection, the harvested cells (2×10^5 in 1 mL) were suspended in 0.5 mL of complete medium containing 10.0 μg/mL of JC-1 for 30 min at 37 °C. JC-1 is a cationic dye that exhibits potential-dependent accumulation in mitochondria, indicated by a fluorescence emission shift from green (525 ± 10 nm) to red (610 ± 10 nm). Cells were observed under a fluorescence microscope (Leica DMIL) according to their color and structure [16].

For apoptotic nuclei analysis, cells were labeled with fluorescent DNA-binding dyes AO/EB double staining, enabling us to perform high-quality studies of cell morphology, nuclear and chromatin disintegration as well as to distinguish viable, early or late apoptotic and necrotic cells [17,18]. Briefly, cells were harvested and washed with PBS after the treatment with 0.8 μmol/L of XJW20 or DMSO for 24 or 48 h, stained with 100 μg/mL AO/EB for 5 min. Then cells were observed under a fluorescence microscope (Leica DMIL) according to the color and structure of nuclei.

For DAPI staining, cells were treated with 0.2–0.8 μmol/L of XJE20 for 48 h and suspended in PBS containing 0.1% Triton X-100 (for increase permeability) and incubated for 10 min on ice. The cells were spun down and resuspended at 5000 cells/well in 4% PBS buffered paraformaldehyde solution containing 0.1 μg/mL DAPI. The nuclei were observed using a fluorescence microscope (Leica DMIL) at excitation wavelength 350 nm. Nuclei showed clear brightly condensed (pycnotic) chromatin or fragmented nuclei were scored as apoptotic cells. A minimum of 500 cells was counted in each sample [19].

2.5. Flow cytometric analysis

For cell-cycle analysis, cell lines (1×10^6 cells in 1 mL of medium) were treated with XJW20 for either 12 or 24 h and then fixed with 70% ethanol at −20 °C for at least 12 h. The cells were incubated in RNase A/PBS (100 μg/mL) at 37 °C for 30 min. Intracellular DNA

was labeled with PI (50 μg/mL) and analyzed with a FACSCalibur fluorescence-activated cell sorter (FACS) using CELL Quest software (Becton Dickinson, NJ). The cell-cycle profile was obtained by analyzing 15,000 cells using the ModFIT LT 3.0 program (Becton Dickinson).

For apoptosis analysis, cell lines were stained with JC-1 or AO/EB to differentiate early or late apoptotic cells. Surface exposure of phosphatidylserine on apoptotic cells was measured using an Apo Alert Annexin V-FITC apoptosis detection kit (BD Biosciences Clontech, CA). Cells were treated according to the manufacturer's instructions and determined with a Coulter EPICS Elite flow cytometer (Coulter Corporation). The harvested cells (2×10^6, 1 mL) were resuspended in 0.5 mL complete medium containing 10.0 μg/mL of JC-1 for 30 min at 37 °C. Samples

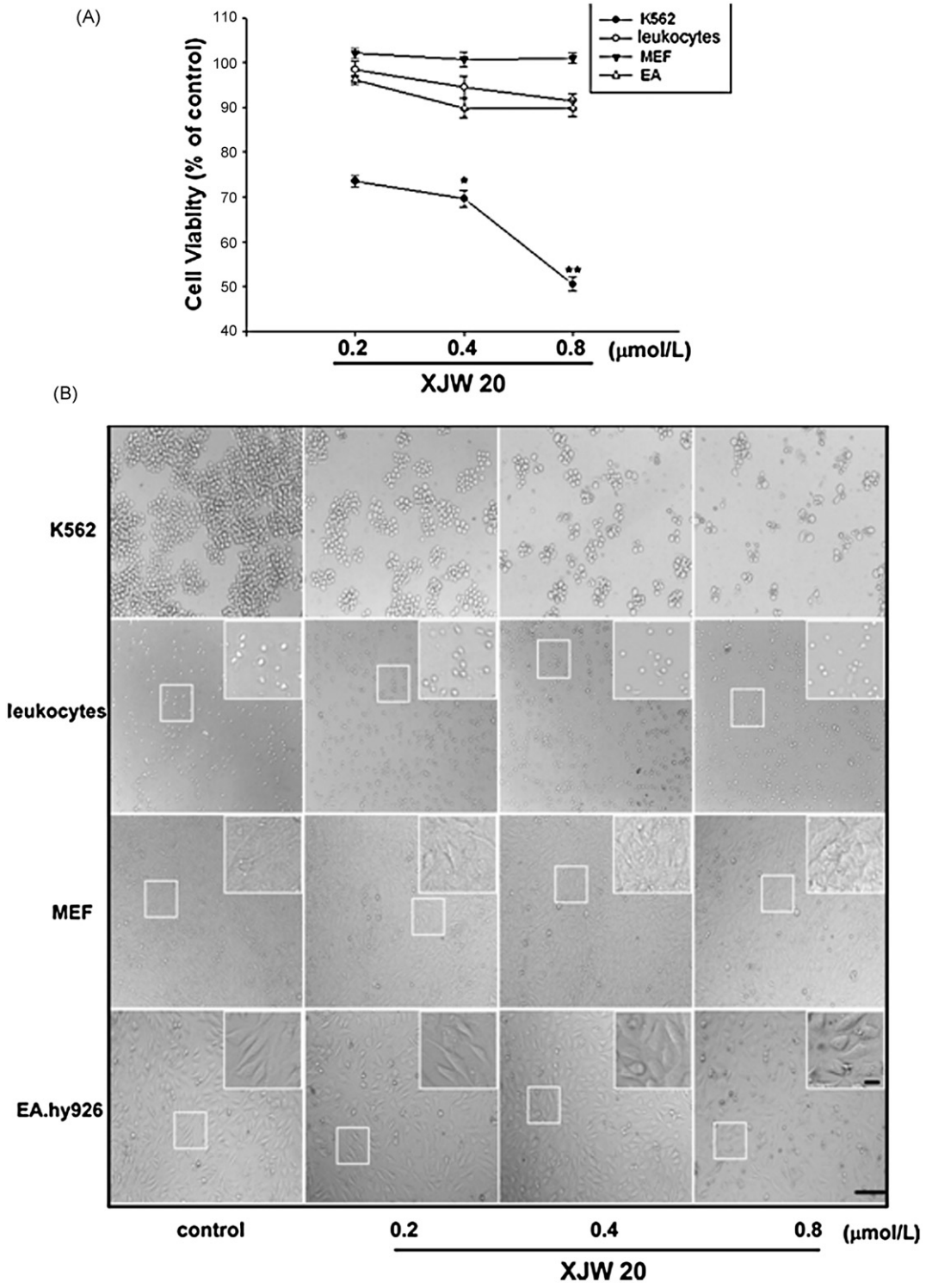

Fig. 2. Cytotoxic effect of XJW20 on leukemic K562 cell line and nontumorous cells. (A) Cytotoxicities were determined by the MTT assay after 48 h of incubation with XJW20 at the indicated concentrations ($n = 3$). (B) Morphological characteristics of cells by phase contrast microscope after 0.2, 0.4, and 0.8 μmol/L XJW20 (2-fold, IC_{50}) treatment for 48 h. It caused significant morphological changes on K562 cell line, but had less effect on the nontumorous cells. DMSO was the negative control. Bar = 100 μm.

(1×10^4cells/sample) were analyzed by FACSCalibur using an argon laser (488 nm). A dot–plot of red fluorescence versus green fluorescence was drawn. Red fluorescence corresponds to living cells with intact mitochondrial $\Delta\Psi_m$ and green fluorescence to cells with lost $\Delta\Psi_m$. Mitochondria depolarization is specifically indicated by a decrease in the red to green fluorescence intensity ratio. Cells were stained with AO/EB final concentration 2 μg/mL for 5 min. Annexin V-PI flow cytometry was analyzed with a Coulter Counter to determine early or late apoptosis.

Table 1
Chronic myeloid leukemia K562 cells were selectively sensitive to proliferation inhibition by the oxoindole derivative XJW20 (72 h treatment), as determined by the MTT assay. Values are averages of at least three independent determinations.

Cell type	IC_{50} (μmol/L, means ± S.D.)
PC-3	51.85 ± 4.87
K562	0.40 ± 0.06
MCF-7	188.10 ± 2.33
A549	>500
HO8910	47.21 ± 5.51

2.6. Western blot analysis

Following treatment, cells were washed with PBS and then lysed with lysis buffer (250 mM Tris–HCl, pH 8, 1% NP-40 and 150 mM NaCl). Equal amounts of extracts were fractionated on a 12% or 15% SDS–polyacrylamide gel. The separated proteins were electrophoretically blotted onto a nitrocellulose membrane (Pierce Biotechnology, Rockford, IL, USA). Blots were incubated with a primary antibody and the secondary horseradish peroxidase-conjugated antibody. Primary antibodies used in this study were against CDK1, CDK2, cyclin B1, p-Cdc25C (Ser216), ERK1/2, p-ERK1/2, cytochrome C (Cytosol) and GAPDH. HRP-labeled secondary anti-mouse or anti-rabbit antibodies were purchased from Santa Cruz Biotechnology (Santa Cruz, CA, USA). The detection reagent ECL was purchased from Israel, Beit, Haemek Ltd. (Kibbutz Beit Haemek, Israel).

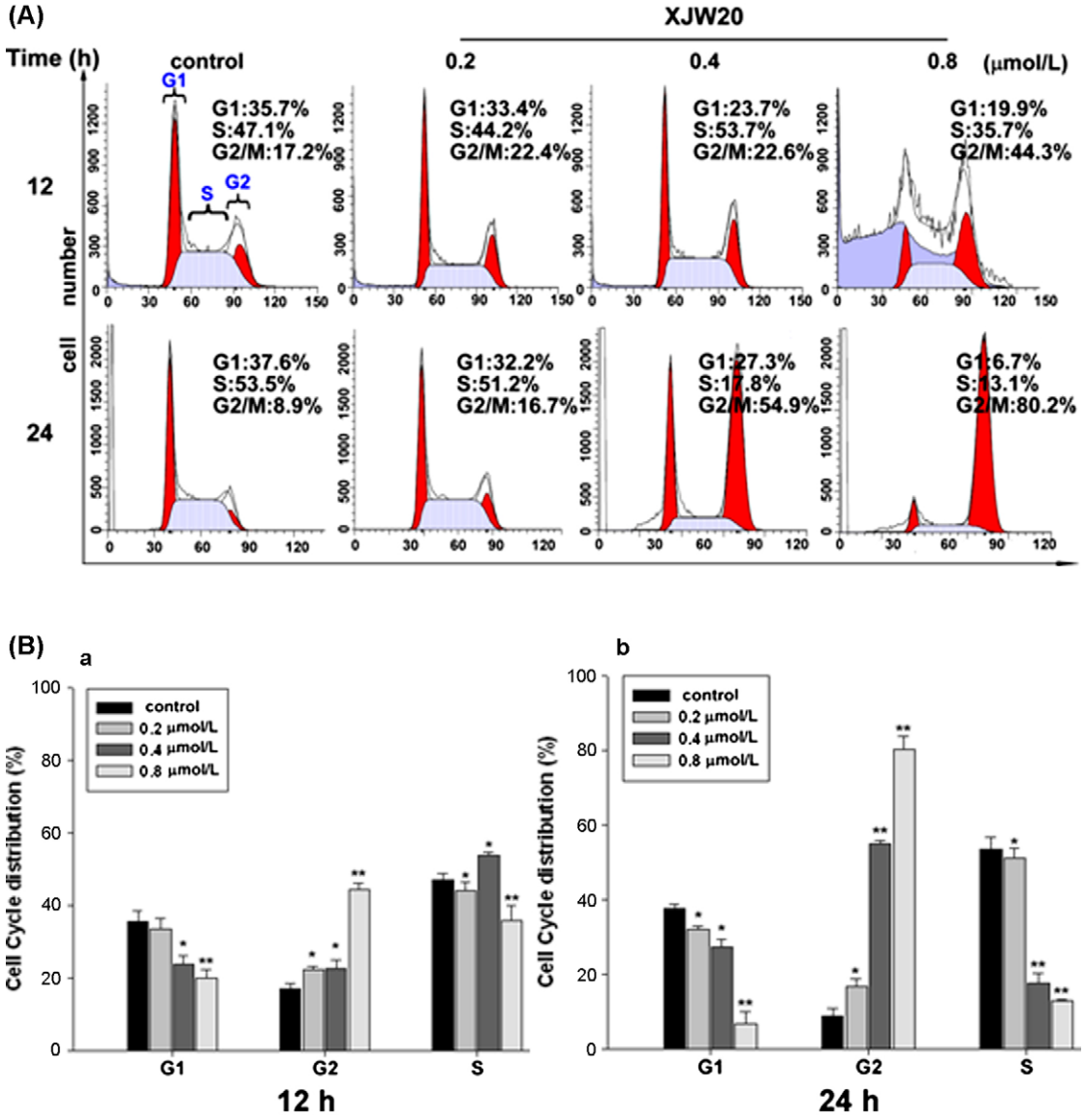

Fig. 3. XJW20 induced G2/M arrest in K562 cells ($n = 3$). (A and B) Cell-cycle distributions after treatment with 0.2, 0.4, and 0.8 μmol/L XJW20 12 or 24 h, DMSO as the negative control. Cell-cycle distributions were assessed by propidium iodide staining. The DNA contents of 15,000 events were analyzed by flow cytometry. (C) Western blot analysis of expressions of CDK1, CDK2, p-Cdc25C, cyclin B1 after treatment with 0.8 μmol/L XJW20 12, 24, 48 h. (D) Western blot analysis of expression of ERK and p-ERK decreased after treatment with 0.8 μmol/L XJW20 1, 2, and 3 h. $^{*}P < 0.05$ and $^{**}P < 0.01$.

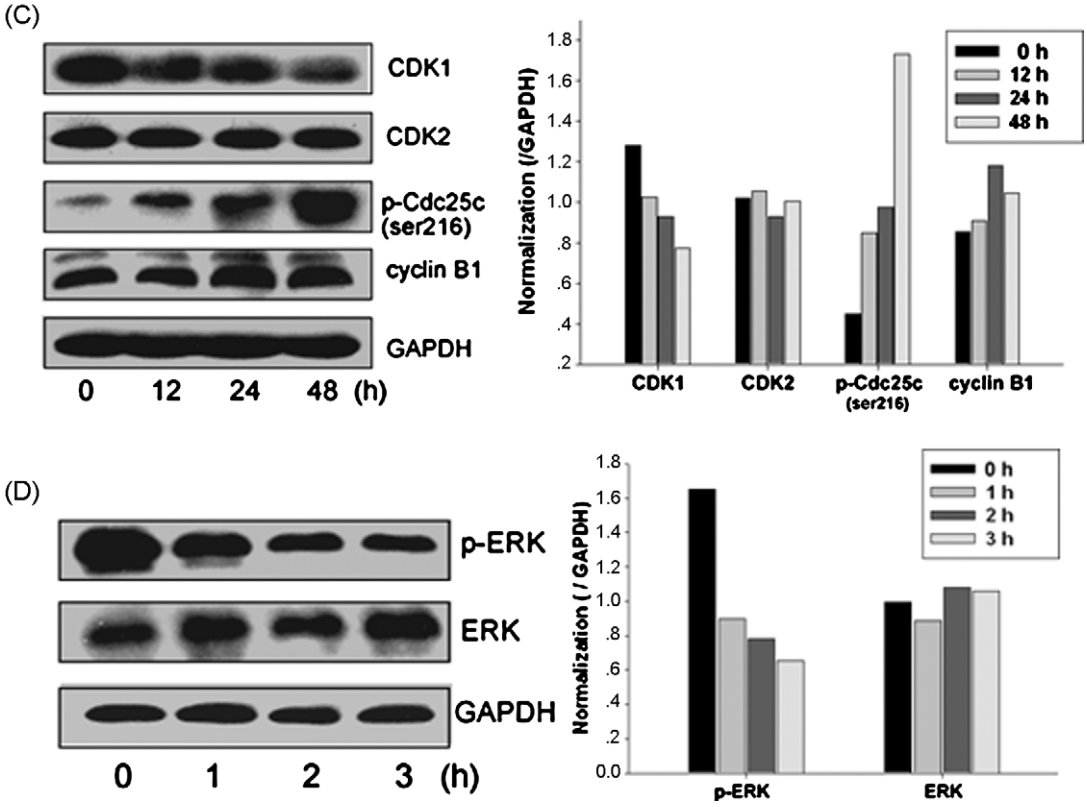

Fig. 3. (*Continued*).

2.7. Detection of intracellular ROS generation

The production of intracellular ROS was measured using the oxidation-sensitive fluorescent dye carboxy-DCFDA. An increase in green fluorescence intensity is used to quantify the generation of intracellular ROS. After adding carboxy-DCFDA at a final concentration of 15 μM to the culture medium, the cells were incubated at 37 °C for an additional 30 min, harvested, washed with PBS, and observed under a fluorescence microscope (Leica DMIL) according to their color and structure or measured immediately with FACSCalibur using an argon laser at 488 nm and a 525-nm band pass filter.

2.8. Statistical analysis

All data were expressed as mean ± S.D. Differences between groups were generally examined for statistical significance using one-way ANOVA analysis with post hoc of Dunnett's test. A *P*-value less than 0.05 denoted a statistically significant difference.

3. Results

3.1. XJW20 has cytotoxic effect on K562 cells

Several cell lines (K562, PC-3, MCF-7, A549, and HO8910) were screened against oxoindole derivate library using MTT

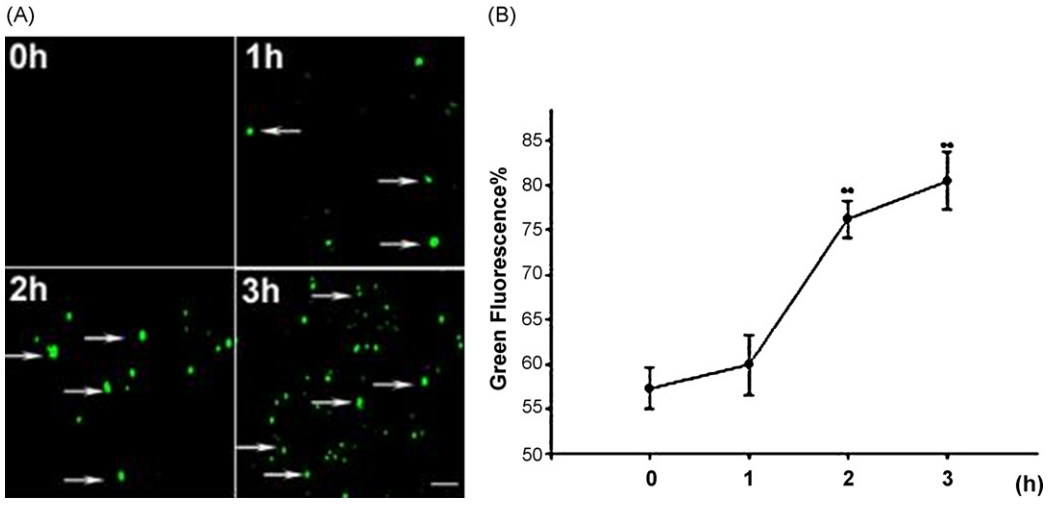

Fig. 4. XJW20 stimulated ROS production in K562 cell line ($n = 3$). Cells were treated with 0.8 μmol/L XJW20 for 1–3 h. DMSO was the negative control. After treatment, cells were washed, and incubated in complete medium containing carboxy-DCFDA for 30 min, and then they were analyzed by (A) fluorescence microscope or (B) flow cytometry.

cell viability assay. After 72 h treatment, XJW20 was found to specifically inhibit the growth of K562 (IC_{50} = 0.40 μM) (Table 1).

To confirm the selected cytotoxic effect, nontumorous cells, such as endothelial cell line, primary cultured MEF and leukocytes, were also evaluated. Cytotoxicity was determined by the MTT test after 48 h of incubation with XJW20. When incubated with XJW20 (0.2–0.8 μM), the growth of K562 cells was markedly inhibited, while the growth rate of other cells were not changed (Fig. 2A). Cell morphology was captured by phase contrast images after treatment with 0.2, 0.4, 0.8 μmol/L of XJW20 48 h (Fig. 2B). The morphological analysis revealed a remarkable difference between XJW20-treated K562 and nontumorous cells.

3.2. XJW20 induces G2/M arrest in K562 cells

Cell-cycle analysis revealed that XJW20 induces G2/M arrest in K562 cells (Fig. 3). As demonstrated in Fig. 3A and B, following 12 h treatment, percentages of G2/M phase cells increased from 17.19% ± 1.45 to 22.40% ± 0.83 (0.2 μM), 22.62% ± 2.38 (0.4 μM), and 44.33% ± 1.96 (0.8uM), respectively. For 24 h treatment, the percentages of G2/M arrested cells were substantially increased from 8.87% ± 2.16 to 16.71% ± 1.99 (0.2 μM), 54.93% ± 0.80 (0.4uM),

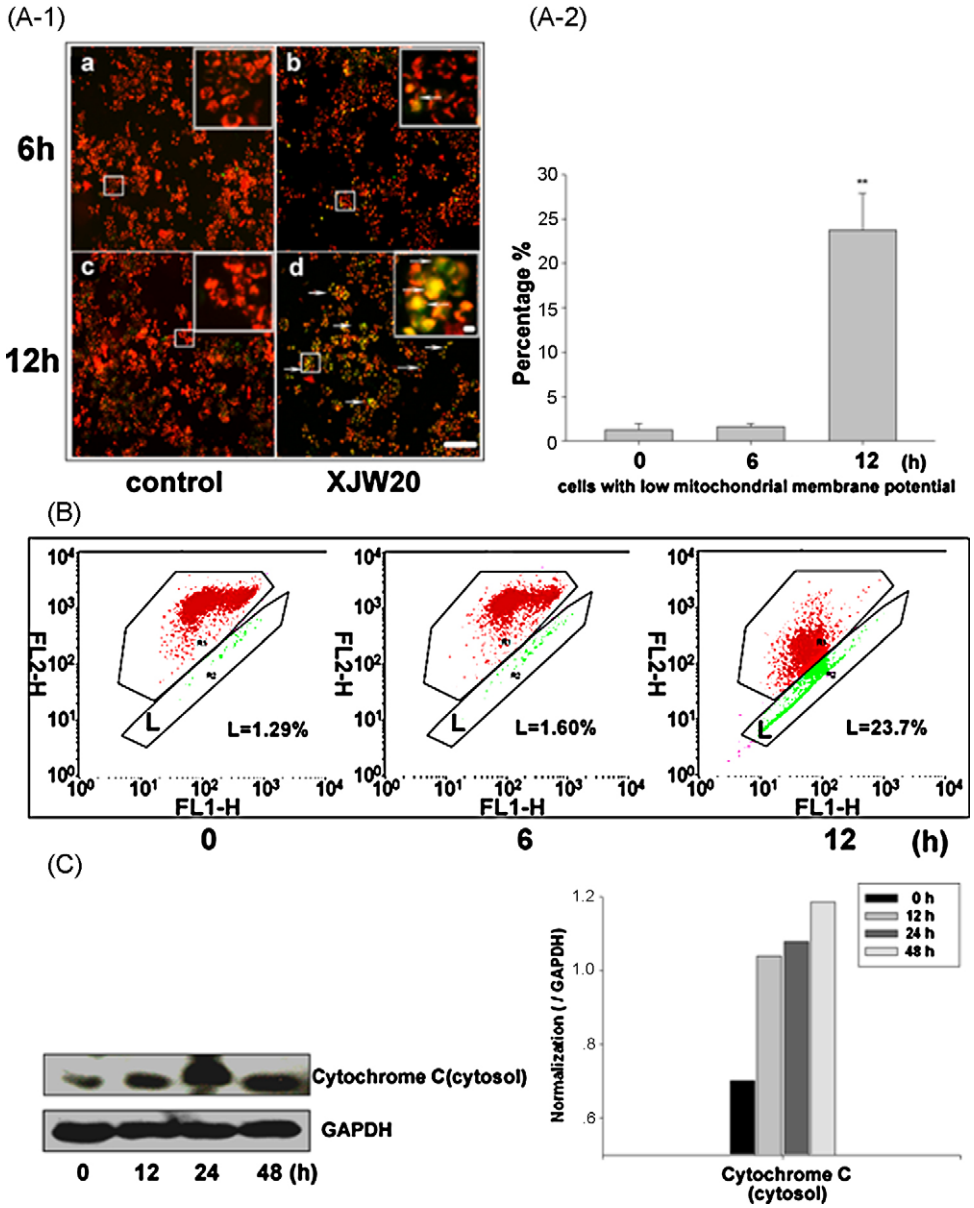

Fig. 5. Mitochondrial membrane potential and cytochrome C release effects of XJW20 on leukemic cell line K562. Cells were treated with or without 0.8 μmol/L XJW20 for 6 or 12 h. (A) The mitochondrial membrane potential ($\Delta\Psi_m$) was measured using the JC-1-staining, in which depolarization is indicated by a switch from the red to green fluorescence intensity. (a and c) Vehicle control and (b and d) exposed to XJW20. (B) A loss of mitochondrial $\Delta\Psi_m$ in cells was detected by flow cytometry. Vehicle incubation 12 h (control) and XJW20 for 6 or 12 h, the green fluorescence intensity indicated the cells with low mitochondrial $\Delta\Psi_m$, while the red one indicated the stable mitochondrial $\Delta\Psi_m$. L: cells with low mitochondrial $\Delta\Psi_m$. (C) Cytochrome C release as affected by XJW20 in K562 cells. (D-1) Fluorescence microscope detection with AO/EB double staining (vital cells with green, and apoptotic cells with orange (early) or red (late) fluorescence intensity); cleft structure of nucli (b and d) or solvent control (a and c). (D-2) Apoptotic cells were determined by Annexin V-PI flow cytometry after DMSO or 0.8 μmol/L of XJW20 treatment for 48 h. (E) Nuclei (DAPI-staining) showed clearly brightly condensed (pycnotic) chromatin or fragmented nuclei were scored as apoptotic cells indicated by *arrows* in (b, c and d). $^{**}P < 0.01$ and Bar = 100 μm. (For interpretation of the references to color in this figure legend, the reader is referred to the web version of the article.)

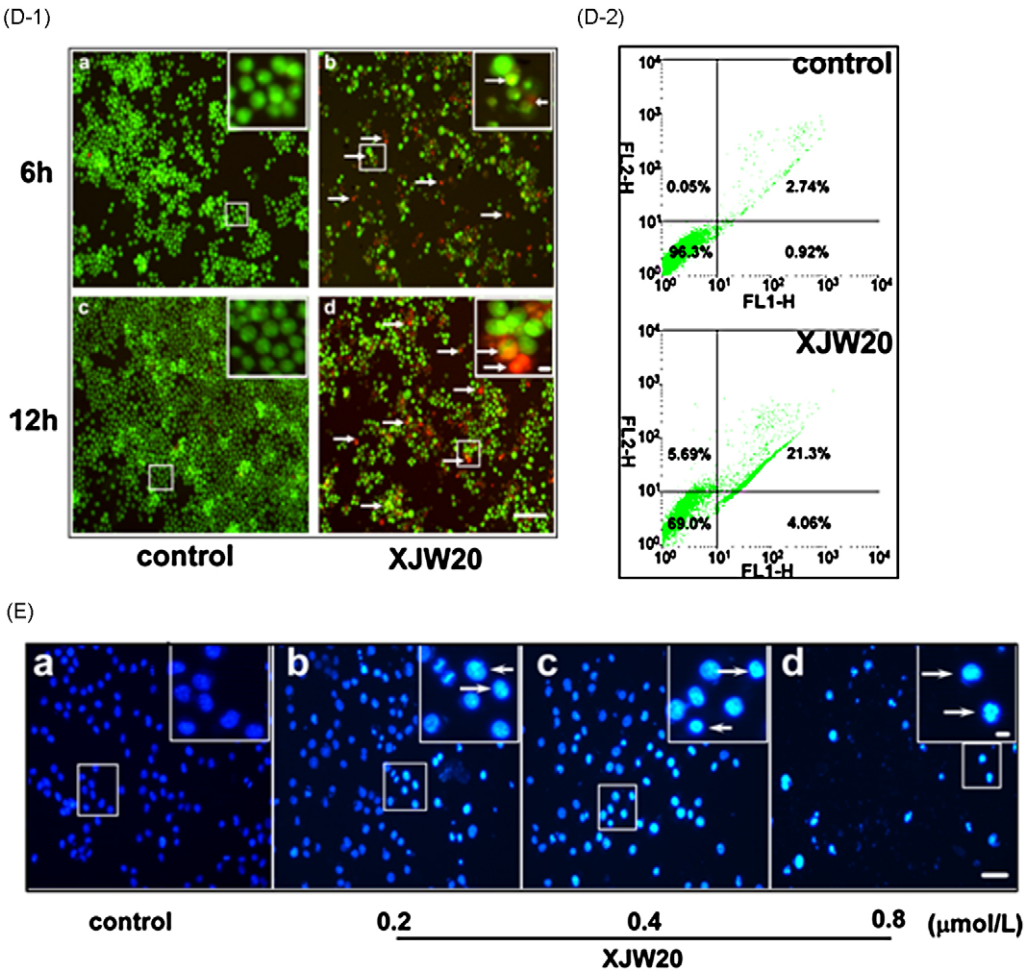

Fig. 5. (*Continued*).

80.23% ± 3.45 (0.8 μM), respectively. These data suggest that XJW20 induces G2/M arrest in a time and concentration-dependent manner.

3.3. XJW20-induced G2/M arrest is accompanied with altered cyclin B1-CDK1 expression and Cdc25C activation

Since cyclin B1-CDK1 is known to be critical for the G2/M transition, its expression levels were determined upon treatment by Western blotting analysis. As shown in Fig. 3C, upon the treatment with 0.8 μM XJW20 for 12, 24, and 48 h, the expression of CDK1 decreased in a time-dependent manner, coinciding with the effective mitotic-arresting process. The amount of p-Cdc25C (ser216), which down-regulates the activity of CDK1, was increased dramatically. There was a modest increase in the expression of cyclin B1 and no change in the expression level of CDK2. These molecular events may contribute to the G2/M arrest induced by XJW20.

3.4. XJW20 induces oxidative stress at early stage

Mitochondria are sensitive to changes in cellular redox state, and ROS can cause mitochondrial dysfunction. K562 cells were treated with 0.8 μM XJW20 for 1–3 h, then stained with carboxy-DCFDA, visualized by a fluorescence microscope (Fig. 4a) and analyzed by flow cytometry (Fig. 4B). The results in Fig. 4 showed that XJW20 could induce generation of ROS in a time-dependent manner.

3.5. XJW20-induced apoptosis is characterized by the mitochondrial transmembrane potential ($\Delta\Psi_m$) dissipation, cytochrome C release, apoptotic nuclei (AO/EB double staining) or nuclei condensation (DAPI-staining)

Cells were treated with 0.8 μM XJW20 for 6 or 12 h, the mitochondrial membrane potential ($\Delta\Psi_m$) was measured using the JC-1-staining. The depolarization is indicated by a switch from the red to green fluorescence intensity. Cells showed more green fluorescence intensity at 12 h than at 6 h (Fig. 5A-1 and A-2). And the loss of mitochondrial membrane potential in cells was confirmed by flow cytometry (Fig. 5B).

To determine whether cytochrome C released was accompanied by altered mitochondria, its expression level was determined by Western blot analysis (Fig. 5C). As shown in Fig. 5C, cytochrome C was released into cytoplasm in a time-dependent manner.

Typical apoptosis features in XJW20-treated cells were observed with AO/EB (Fig. 5D) and DAPI (Fig. 5E). In the case of AO/EB staining, upon treatment with 0.8 μM XJW20, the double staining of the orange or red color and cleft structure of nuclei was seen (Fig. 5D-1). Apoptotosis was further confirmed by Annexin V-PI flow cytometry (Fig. 5D-2). In the case of DAPI staining, 48 h post treatment by 0.2–0.8 μM XJW20, nuclei were condensed (pycnotic) in a concentration-dependent manner (Fig. 5E).

4. Discussion

This study found that XJW20, a novel oxoindole derivative, has selective cytotoxic activity in the chronic myelogenous leukemia K562 cell line, but has hardly any cytotoxicity in several other neoplastic cell lines and myeloid or somatic cell lines. Focusing on cell-cycle progression and apoptosis, the present results demonstrated that G2/M arrest and apoptosis induced by XJW20 might contribute to its cytotoxcity in K562 cells.

Cell-cycle regulation is intricate, and the cell-cycle progression is tightly regulated by the synthesis/degradation, association/dissociation, translocation between cytoplasm and nucleus, and the phosphorylation/dephosphorylation of various protein regulators [5,9]. CDKs are key elements of cell-cycle progression. CDKs and their associated molecule elements have been considered as potential targets for anticancer drug discovery [1–3]. G2/M arrest has been shown to be a protective mechanism that ensures orderly and timely repair of damages and prevents inappropriate mitotic entry. G2/M checkpoint is the most prominent effect of many anticancer agents in tumor cells when they have sustained DNA damages induced by therapeutic agents.

The present results revealed several molecular events, such as ROS generation, phosphorylation of ERK1/2, phosphorylation states of Cdc25C, and expression of CDK1, involved in the mechanism of XJW20-induced G2/M arrest may change the mode of signal transduction after survival promotion pathway, and ERK MAP kinase is directly involved in activating Cdc25C during the G2/M transition (11).

Chemotherapy-induced oxidative stress is one of the mechanisms that kills cancer cells [20]. Kinetics studies revealed that ROS generation and phosphorylated ERK down-regulation appeared in XJW20-treated K562 cells simultaneously. As tumor cells are actively engaged in energy metabolism and ROS generation during energy metabolism, cells are more dependent on the essential enzyme superoxide dismutase to protect cells from oxidative damage by converting superoxide anion to H_2O_2, and followed by catalase to H_2O. Excessive ROS generation may change the mode of signaling transduction in the cells after treatment with XJW20. The MAPK pathway has been implicated in the response of tumor cells to chemotherapeutic drugs, such as taxol, etoposide and cisplatin, suggesting that the MAPK pathway may be a promising target for anticancer drugs. It has been reported that JNK plays an important role in IQDMA-mediated G2/M arrest and apoptosis of K562 cancer cells [21]. The ERK pathway is generally considered as a survival promotion pathway and ERK MAP kinase is directly involved in activating Cdc25C during the G2/M transition [11]. Down-regulation of phosphorylated ERK should determine K562 cell fate after exposure to XJW20.

Compounds with an oxoindole parent structure were expected to selectively regulate CDKs [4,5]. This study showed down-regulation of CDK1 and up-regulation of phosphorylated Cdc25C in XJW20-treated K562 cells, which could contribute to G2/M arrest. However, there was no change in the expression of CDK2 in XJW20-treated K562 cells. Inhibition of CDK1 and CDK2 frequently results in arrest at the G1/S and G/M boundaries. CDK1 inhibition may especially augment cell death after mitotic checkpoint activation by taxanes, but highly selective CDK2 inhibition does not have antiproliferative effects in many cancer cell types [1]. With XJW20-treatment, the G2/M arrest was accompanied with the increase in cyclin B1. Since the activity of Cdc25C is negatively regulated by phosphorylation of Cdc25C on the serine-216 residue [8,9], we evaluated the phosphorylation states of Cdc25C in K562 cells after treatment with XJW20. One of the network-complexes that regulate the G2 to M transition has been revealed to be a Cdc25C-cyclin B1/Cdc2 controlled switch-like system [9]. At the onset of mitosis, the complexes of cyclin B1/Cdc2 become active when the dual specificity phosphatase, Cdc25C, removes inhibitory phosphorylations on Cdc2. Once active the cyclin B1/Cdc2 complexes phosphorylate Cdc25C, which enhances its phosphatase activity [22]. This study suggested that G2/M arrest in k562 cells treated with XJW20 was related to an increase in cyclin B1 expression and phospho (p)-Cdc25C (Ser216) activation, as well as a decrease in CDK1 expression. Thus, we presumed that fast growth and short cell cycle might contribute to K562 cells for the high sensitivity to XJW20.

Intracellular ROS generation increased in K-562 cells with XJW20 treatment, which may have participated in a set of responses that lead to apoptosis through enhanced intracellular ROS [12], driving the cell to an oxidative stress-induced cell death. Consistent with previous reports [16,20], XJW20 induced apoptosis was characterized by mitochondrial $\Delta\Psi_m$ dissipation, cytochrome C release apoptotic nuclei formation and nuclei condensation.

Apoptosis can be exerted through two different signaling pathways, namely the mitochondrial pathway and the cell death receptor pathway. Preservation of the mitochondrial $\Delta\Psi_m$ was crucial for the prevention of photoreceptor apoptosis; its loss was parallel to the increase in photoreceptor apoptosis during early development *in vitro* and upon oxidative damage. The key element in the mitochondrial pathway is the efflux of cytochrome C from the mitochondria to the cytosol. Once cytochrome C is released into the cytosol, cytochrome C together with Apaf-1 activates caspase-9, and the latter then activates caspase-3. XJW20 treatment induced a decrease of mitochondrial $\Delta\Psi_m$ at an early treatment stage, which might associate with K562 cell apoptosis. Cytochrome C release is a hallmark of mitochondrial dysfunction, and XJW20 could induce the release of cytochrome C after the mitochondrial $\Delta\Psi_m$ decreases. This further confirmed that XJW20-induced apoptosis in K562 cells occurs through the mitochondrial pathway.

Furthermore, we used AO/EB staining, which allows the identification of viable, apoptotic and necrotic cells based on color and

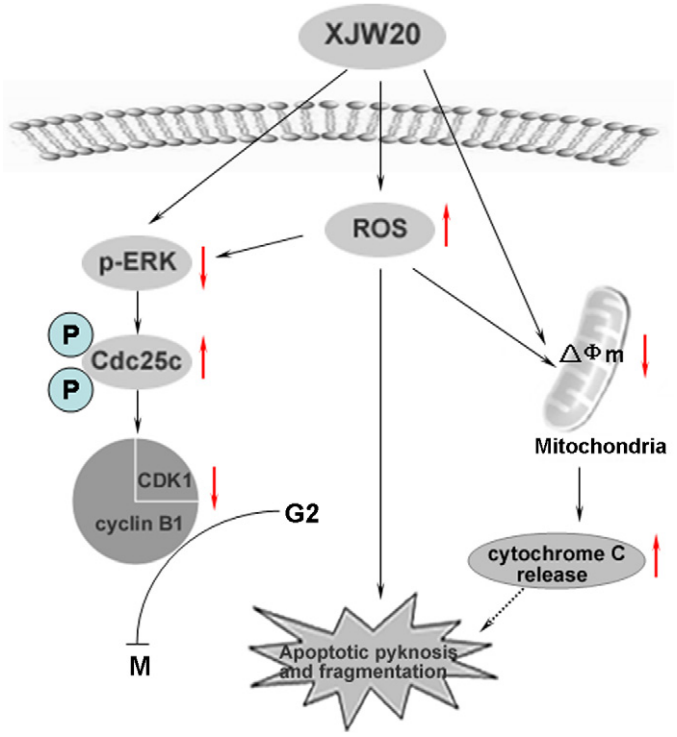

Fig. 6. Schematic drawing with proposed mechanisms by which XJW20 can arrest proliferation of K562 cells. The cartoon compiles the results and conclusions of this report. The cartoon compiles the results and conclusions of this report.

appearance. Our data confirmed an induction of apoptotic death in XJW20-treated K562 cells. It could be of significance in identifying another anticancer mechanism (together with the cell-cycle arrest) of XJW20. That is, the novel CDK inhibitor also caused apoptosis in K562 cells. The multiple targets of XJW20 may play an essential role in enhancing efficiency in K562 cells and reducing chemoresistance in CML chemotherapy.

In conclusion, our study demonstrated that the cytotoxic effect of XJW20 in K562 cell line appears to be through G2/M phase arrests and intracellular apoptosis. XJW20 inhibited cell growth of K562 cells, arrested cell cycle with alteration in phosphorylated ERK, phosphorylated Cdc25C, CDK1 protein expression. Decreased mitochondrial $\Delta\Psi_m$, and ROS induction at a much earlier stage possibly played an important role in XJW20 induced apoptosis (Fig. 6). XJW20 could be a potentially effective therapeutic target against CML cells for further study.

Conflict of interest statement

None.

Acknowledgment

This work was supported in part by National Natural Sciences Foundation of China (No. 30672564 and No. 30772652).

References

[1] G.I. Shapiro, Cyclin-dependent kinase pathways as targets for cancer treatment, J. Clin. Oncol. 24 (2006) 1770–1783.
[2] E.A. Sausville, Complexities in the development of cyclin-dependent kinase inhibitor drugs, Trends Mol. Med. 8 (4 Suppl.) (2002) S32–37.
[3] I. Diaz-Padilla, L.L. Siu, I. Duran, Cyclin-dependent kinase inhibitors as potential targeted anticancer agents, Invest. New Drugs (2009), doi:10.1007/s10637-009-9236-6.
[4] K.C. Luk, M.E. Simcox, A. Schutt, K. Rowan, T. Thompson, Y. Chen, U. Kammlott, W. Depinto, P. Dunten, A. Dermatakis, A new series of potent oxindole inhibitors of CDK2, Bioorg. Med. Chem. Lett. 14 (2004) 913–917.
[5] A. Dermatakis, K.C. Luk, W. DePinto, Synthesis of potent oxindole CDK2 inhibitors, Bioorg. Med. Chem. 11 (2003) 1873–1881.
[6] B. Funari, N. Rhind, P. Russell, Cdc25 mitotic inducer targeted by chk1 NA damage checkpoint kinase, Science 277 (1997) 1450–1451.
[7] B.D. Aguda, A quantitative analysis of the kinetics of the G(2) DNA damage checkpoint system, Proc. Natl. Acad. Sci. U.S.A. 96 (1999) 11352–11357.
[8] H.L. Chang, Y.C. Wu, J.H. Su, Y.T. Yeh, S.S. Yuan, Protoapigenone, a novel flavonoid, induces apoptosis in human prostate cancer cells through activation of p38 mitogen-activated protein kinase and c-Jun NH2-terminalkinase 1/2, J. Pharmacol. Exp. Ther. 325 (2008) 841–849.
[9] L. Yan, J.R. Donze, L. Liu, Inactivated MGMT by O^6-benzylguanine is associated with prolonged G2/M arrest in cancer cells treated with BCNU, Oncogene 24 (2005) 2175–2183.
[10] D. Cai, V.M. Latham, X. Zhang, G.I. Shapiro, Combined depletion of cell cycle and transcriptional cyclin-dependent kinase activities induces apoptosis in cancer cells, Cancer Res. 66 (2006) 9270–9280.
[11] R. Wang, G. He, M. Nelman-Gonzalez, C.L. Ashorn, G.E. Gallick, P.T. Stukenberg, M.W. Kirschner, J. Kuang, Regulation of Cdc25C by ERK-MAP kinases during G2/M transition, Cell 128 (2007) 1119–1132.
[12] R.R. Rosato, J.A. Almenara, S. Grant, The histone deacetylase inhibitor MS-275 promotes differentiation or apoptosis in human leukemia cells through a process regulated by generation of reactive oxygen species and induction of p21CIP1/WAF1, Cancer Res. 63 (2003) 3637–3645.
[13] B.A. van Oost, C.J. Edgell, C.W. Hay, R.T. MacGillivray, Isolation of human von Willebrand factor cDNA from the EA.hy926 cell line, Biochem. Cell Biol. 64 (1986) 699–705.
[14] I. Wilmut, L. Young, K.H. Campbell, Embryonic and somatic cell cloning, Reprod. Fertil. Dev. 10 (1998) 639–643.
[15] S.H. Su, S.J. Su, S.R. Lin, K.L. Chang, Cardiotoxin III selectively enhances activation-induced apoptosis of human CD8+ T lymphocytes, Toxicol. Appl. Pharmacol. 193 (2003) 97–105.
[16] T. Zuliani, R. Duval, C. Jayat, S. Schnébert, P. André, M. Dumas, M.H. Ratinaud, Sensitive and reliable JC-1 and TOTO-3 double staining to assess mitochondrial transmembrane potential and plasma membrane integrity: interest for cell death investigations, Cytometry A 54 (2003) 100–108.
[17] D.L. Pitrak, H.C. Tsai, K.M. Mullane, S.H. Sutton, P. Stevens, Accelerated neutrophil apoptosis in the acquired immunodeficiency syndrome, J Clin. Invest. 98 (1996) 2714–2719.
[18] D. Baskić, S. Popović, P. Ristić, N.N. Arsenijević, Analysis of cycloheximide-induced apoptosis in human leukocytes: fluorescence microscopy using annexin V/propidium iodide versus acridin orange/ethidium bromide, Cell Biol. Int. 30 (2006) 924–932.
[19] R.L. Dusek, S. Getsios, F. Chen, J.K. Park, E.V. Amargo, V.L. Cryns, K.J. Green, The differentiation-dependent desmosomal cadherin desmoglein 1 is a novel caspase-3 target that regulates apoptosis in keratinocytes, J. Biol. Chem. 281 (2006) 3614–3624.
[20] Y.H. Ling, L. Liebes, Y. Zou, R. Perez-Soler, Reactive oxygen species generation and mitochondrial dysfunction in the apoptotic response to Bortezomib, a novel proteasome inhibitor, in human H460 non-small cell lung cancer cells, J. Biol. Chem. 278 (2003) 33714–33723.
[21] S.H. Yang, C.M. Chien, C.M. Lu, Y.L. Chen, L.S. Chang, S.R. Lin, Involvement of c-Jun N-terminal kinase in G2/M arrest and FasL-mediated apoptosis induced by a novel indoloquinoline derivative, IQDMA, in K562 cells, Leuk. Res. 31 (2007) 1413–1420.
[22] E. Villa-Moruzzi, Activation of the Cdc25C phosphatase in mitotic Hela cells, Biochem. Biophys. Res. Commun. 196 (1996) 1248–1254.